BIOCHEMISTRY
including biophysical chemistry & molecular biology
Article

Biochemistry **2011,** *50,* 1545–1555 1545
DOI: 10.1021/bi101455b

Mutational Analysis of Catecholamine Binding in Tyrosine Hydroxylase[†]

Gabrielle D. Briggs, Sarah L. Gordon,[‡] and Phillip W. Dickson*

The School of Biomedical Sciences and Pharmacy and The Hunter Medical Research Institute, Faculty of Health, The University of Newcastle, Callaghan, New South Wales 2308, Australia. [‡]Current address: Centre for Integrative Physiology, The University of Edinburgh, Edinburgh, U.K.

Received September 8, 2010; Revised Manuscript Received January 13, 2011

ABSTRACT: Tyrosine hydroxylase (TH) performs the first and rate-limiting step in the synthesis of catecholamines, which feed back to regulate the enzyme by irreversibly binding to a high-affinity site and inhibiting TH activity. Phosphorylation of Ser40 relieves this inhibition by allowing dissociation of catecholamine. We have recently documented the existence of a low-affinity catecholamine binding which is dissociable, is not abolished by phosphorylation, and inhibits TH by competing with the essential cofactor, tetrahydrobiopterin. Here, we have substituted a number of active site residues to determine the structural nature of the low- and high-affinity sites. E332D and Y371F increased the IC_{50} of dopamine for the low-affinity site 10-fold and 7 0-fold, respectively, in phosphorylated TH, indicating dramatic reductions in affinity. Only 2−4-fold increases in IC_{50} were measured in the nonphosphorylated forms of E332D and Y371F and also in L294A and F300Y. This suggests that while the magnitude of low-affinity site inhibition in wild-type TH remains the same upon TH phosphorylation as previously shown, the active site structure changes to place greater importance on E332 and Y371. Changes to high affinity binding were also measured, including a loss of competition with tetrahydrobiopterin for E332D, A297L, and Y371F and a decreased ability to inhibit catalysis (V_{max}) for A297L and Y371F. The common roles of E332 and Y371 indicate that the low- and high-affinity catecholamine binding sites are colocalized in the active site, but due to simultaneous binding, may exist in separate monomers of the TH tetramer.

The enzyme, tyrosine hydroxylase (TH),[1] catalyzes the first and rate-limiting step in the synthesis of the catecholamines, adrenaline, noradrenaline, and dopamine. This reaction occurs in catecholaminergic neurons and adrenal chromaffin cells and involves the cytosolic conversion of tyrosine to the dopamine precursor, L-DOPA. This occurs in a 17 Å deep catalytic cleft comprised mainly of protein side chains, three making monodentate coordinations with an atom of iron (*1*). Hydroxylation of tyrosine involves the initial binding of an essential cofactor tetrahydrobiopterin (BH_4) to the active site, which subsequently donates electrons to ferrous iron [Fe(II)], producing a ferryl-oxo species [Fe(IV)O] in the presence of molecular oxygen (*2*, *3*). Fe(IV)O subsequently interacts with the aromatic ring of bound tyrosine to hydroxylate the carbon at the 3 position, producing L-DOPA. In addition to the catalytic core, TH consists of an N-terminal regulatory domain of 156 amino acids containing phosphorylation sites at serines 8, 19, 31, and 40 (*4*). This region is thought to be highly flexible, and attempts to define the N-terminus in crystal structures have been unsuccessful thus far. The TH quaternary structure in native and recombinant forms has been described as a dimer of dimers, with the catalytic domains of TH monomers associating via a salt bridge and resultant pairs of dimers inter-acting to form an antiparallel leucine zipper core from their C-terminal domains (*1*).

Being the rate-limiting enzyme in catecholamine biosynthesis, TH is tightly regulated by a number of mechanisms ranging from transcriptional regulation and RNA stability to substrate inhibition and phosphorylation (*5*). One of the most striking mechanisms for short-term regulation of TH involves end point feedback inhibition by the catecholamines which bind irreversibly and covalently to the catalytic iron in the active site (*6*), trapping it in a ferric [Fe(III)] form. The effect of this high-affinity binding on TH activity is twofold: the maximal velocity (V_{max}) of the reaction is greatly reduced to approximately 3% of the activity in the absence of catecholamine (*7*, *8*), and the bound catecholamine additionally disrupts binding of the cofactor, measured in a kinetic analysis as an increase in the Michaelis constant (K_M) for BH_4 of up to 100-fold (*8*). This inhibition is relieved only by phosphorylation of the Ser40 residue in the regulatory domain (*9*), allowing the bound catecholamine to dissociate(*10*). Thus, in catecholaminergic neurons and adrenal chromaffin cells, TH is considered to be in a low activity state until activated by kinases such as cAMP-dependent protein kinase, protein kinase C, or calcium/calmodulin-dependent protein kinase (*5*). However, the existence of a simultaneous, low-affinity catecholamine binding has recently been shown, which differs from the aforementioned high-affinity site in that the binding is dissociable and is not abolished by phosphorylation (*8*). In binding to the low-affinity site, catecholamines have been shown to regulate TH activity *in vitro* (*8*) and *in situ* (*11*) by dissociating and rebinding in response to changes in catecholamine levels and thus may have a role *in vivo* of controlling the availability of cytosolic catecholamines under basal conditions. Additionally, inhibition of TH through this site would constitute the only control point by catecholamines in phosphorylated TH and so may serve as an important regulat-

[†]This work was supported by a grant from the National Health and Medical Research Council (No. 455547).

*Corresponding author. Tel: (612) 4921-7031. Fax: (612) 4921-6903. E-mail: phil.dickson@newcastle.edu.au.

[1]Abbreviations: TH, tyrosine hydroxylase; Ser, serine; PKA, cAMP-dependent protein kinase; BH_4, tetrahydrobiopterin; OC, ovalbumin-coated; K_M, Michaelis constant; V_{max}, maximal velocity; IC_{50}, concentration required to reach 50% inhibition; K_D, dissociation constant; B_{max}, maximal binding.

Published on Web 01/14/2011

ory mechanism when TH is activated. Like the high-affinity site, the low-affinity site inhibits TH by competing with BH_4 but does not decrease the maximal velocity of the reaction (*8*).

High- and low-affinity catecholamine inhibition of TH has been functionally characterized previously; however, what remains to be elucidated are the structural elements which produce these two binding sites. The high-affinity catecholamine binding site has been localized to the active site of TH due to its proven interaction with iron (*6*). Furthermore, localization of catecholamine to this restricted area would likely result in an overlap with the BH_4 binding site, accounting for its disruption of cofactor binding. The location of the low-affinity site has not yet been defined; however, it is likely to involve active site binding due to its effect on the cofactor. The common effect of the high- and low-affinity sites on the cofactor raises the possibility that these two sites occupy a similar region of the active site, and yet their other properties are vastly different. What structural elements, then, account for these differences? To answer this question, active site residues were substituted to determine whether the high- and low-affinity sites involve the same set of residues or whether the two sites are structurally unrelated. The cofactor-bound TH crystal structure (PDB: 2TOH) (*12*) was examined to select candidate amino acids whose side chains protruded into the catalytic cleft, and substitutions were then chosen with the aim of disrupting and structurally separating the two types of catecholamine binding in human TH.

MATERIALS AND METHODS

Materials. For site-directed mutagenesis, reagents and XL1-Blue cells were supplied in the QuikChange II site-directed mutagenesis kit from Stratagene (La Jolla, CA), and oligonucleotides were supplied by GeneWorks (Hindmarsh, Australia). Plasmid purification used the QuickLyse miniprep kit provided by Qiagen (Hilden, Germany). Bacterial protein expression used BL21 DE-3 cells supplied by Invitrogen (Carlsbad, CA). Heparin Sepharose and 3,5-[^{3}H]-L-tyrosine were provided by GE Healthcare (Little Chalfont, U.K.). Tetrahydrobiopterin was supplied by Dr. Schirck's Laboratory (Jona, Switzerland). L-Tyrosine was supplied by BDH Biochemicals (Poole, U.K.). PKA from bovine heart, catalase, reduced glutathione, activated charcoal, ovalbumin, and dopamine hydrochloride were supplied by Sigma-Aldrich (St. Louis, MO). [2,5,6-^{3}H]Dopamine and Optiphase HiSafe scintillation cocktail were provided by Perkin-Elmer (Waltham, MA).

Generation, Expression, and Purification of Active Site Mutants. Site-directed mutagenesis using the oligonucleotides shown in Table 1 was performed on a pET3a vector containing the human TH isoform 1 cDNA (NM_000360.3) as a wild-type template. Mutagenesis was carried out using the QuikChange II site-directed mutagenesis kit (Stratagene) according to manufacturer's instructions. Transformation of *Dpn*I-digested PCR products into *Escherichia coli* (XL1-Blue supercompetent cells from Stratagene) was performed using heat shock at 42 °C and growth for 1 h at 37 °C in LB medium. Transformed bacteria were grown on 100 μg/mL ampicillin-containing LB agar at 37 °C overnight. After the presence of mutations was confirmed by DNA sequencing, BL21 DE-3 was transformed with plasmid purified from XL1-Blue transformants as above.

Wild-type TH, L294A, E332Q, and E332D were expressed in BL21 DE-3 using previously described methods (*9*, *13*). For L294Y, A297L, F300A, F300Y, and Y371F, bacteria were grown at 37 °C with shaking until an optical density of 0.6 was reached, upon which they were transferred to 22 °C until the temperature equilibrated and an optical density of 0.8 was reached. Isopropyl β-D-1-thiogalactopyranoside (50 mM) was then added to induce protein expression, and bacteria were grown overnight at 22 °C. Wild-type and mutant TH were purified using heparin Sepharose chromatography as previously described (*9*).

Table 1: Mutant Oligonucleotides Used for Site-Directed Mutagenesis[a]

substitution	oligonucleotide (5′−3′)
L294A	CCTGTGGCCGGC**GC**G**C**TGTCCGCCCG
L294Y	GCCTGTGGCCGGC**TAT**CTGTCCGCCCGGG
A297L	GTCCGCCCGGGAC**GCC**CTGGCCAGCCTG
F300A	CCGGCCTGCTGTCC**CTA**CGGGACTTCCTGGC
F300Y	TCCGCCCGGGAC**TAT**CTGGCCAGCCTGG
E332Q	GACTGCTGCCAC**CAG**CTGCTGGGGC
E332D	CTGCTGCCACGA**TCT**GCTGGGGCAC
Y371F	GCTGTCCACGCTG**TTC**TGGTTCACGGTGG

[a]Oligonucleotides are shown for the coding strand (forward primers). Bold letters indicate the mutant codon while underlined letters represent the base changes.

Protein concentrations were determined by SDS−PAGE and Coomassie staining comparing TH samples to standard concentrations of bovine serum albumin.

TH Phosphorylation by PKA. The phosphorylation reaction included up to 7 μM purified TH, between 0.05 and 0.2 units/μL PKA depending on the TH concentration used, 0.5 mM ATP, 12.5 mM $MgCl_2$, and 50 mM Tris, pH 7.4. Addition of PKA initiated the phosphorylation reaction, which proceeded for up to 30 min at 30 °C. TH phosphorylation was carried out immediately prior to its use in activity assays.

Inhibition of TH by Dopamine. Dopamine hydrochloride was dissolved in 5 mM HCl to minimize oxidation and placed on ice until required. For dose−response experiments, suitable amounts of phosphorylated or nonphosphorylated TH were incubated with 0.002−500 μM dopamine for 20 min prior to TH activity assays. For kinetic analyses carried out in the presence of dopamine, suitable amounts of phosphorylated or nonphosphorylated TH were incubated with 10 μM dopamine for 20 min prior to TH activity assays. For those mutants showing decreased affinities for dopamine (higher IC_{50} values), the amount of dopamine used in kinetic analyses was increased proportionally to the change in IC_{50} to ensure saturating conditions. All dopamine incubations were carried out in the presence of 5 mM reduced glutathione to prevent dopamine oxidation and 100 mM potassium phosphate, pH 7.2.

Isolation of High-Affinity Dopamine-Bound TH. Ovalbumin-coated (OC) charcoal was used to prepare samples of TH containing dopamine bound to the high-affinity site alone. By coating in ovalbumin, charcoal has been previously shown to successfully bind and remove free and TH-dissociable dopamine from solution while leaving TH active, intact, and in solution (*8*). OC charcoal was prepared by activating charcoal with 1 M HCl followed by neutralization by sequential washes of H_2O, 0.5 M HEPES, 50 mM HEPES, and 50 mM potassium phosphate (all buffers, pH 7.2). Activated charcoal was centrifuged at 18000*g* at 4 °C for 10 min, supernatant removed, and charcoal resuspended in 40 mg/mL ovabumin, 0.06 mg/mL catalase, and 1.5 mg/mL reduced glutathione in 100 mM potassium phosphate, pH 7.2, to a final charcoal content of 2% (w/v). The slurry was incubated at room temperature with shaking for 1 h to allow the ovalbumin to coat the charcoal. The mixture was then centrifuged at 18000*g* at

Table 2: Kinetic Parameters of Wild-Type and Mutant TH[a]

	nonphosphorylated			phosphorylated		
enzyme	$K_{M\,BH_4}$ (μM)	V_{max} (min^{-1})	V/K (μM^{-1} min^{-1})	$K_{M\,BH_4}$ (μM)	V_{max} (min^{-1})	V/K (μM^{-1} min^{-1})
wild type	14 ± 1	35 ± 3	2.74 ± 0.31	5.6 ± 1.0	28 ± 0.9	5.36 ± 0.99
L294A	14 ± 0.5	11 ± 0.2**	0.78 ± 0.01**	29 ± 1***	8.5 ± 0.6***	0.30 ± 0.04**
L294Y	15 ± 0.4	7.1 ± 0.04***	0.46 ± 0.01**	9.9 ± 0.6*	4.1 ± 0.2***	0.42 ± 0.04**
A297L	20 ± 1**	16 ± 0.4**	0.82 ± 0.02**	17 ± 0.2***	13 ± 0.2**	0.75 ± 0.001**
F300A	54 ± 3***	5.3 ± 0.15***	0.10 ± 0.01***	70 ± 2***	6.7 ± 0.3***	0.10 ± 0.002**
F300Y	26 ± 0.8***	18 ± 0.6**	0.67 ± 0.002**	12 ± 1**	16 ± 0.6**	1.31 ± 0.05*
E332Q						
E332D	8.3 ± 0.3**	3.6 ± 0.1***	0.44 ± 0.02**	7.2 ± 0.4	2.8 ± 0.2***	0.39 ± 0.02**
Y371F	17 ± 1	12 ± 0.3**	0.70 ± 0.03**	29 ± 4**	18 ± 1*	0.64 ± 0.06**

[a]Kinetic parameters were calculated from TH activity assays conducted over 0−200 μM BH_4. Values shown represent the mean ± SEM (N = 3). Asterisks represent significant differences between wild-type and mutant parameters as measured using Student's t test: *, $p < 0.05$; **, $p < 0.01$; ***, $p < 0.001$.

4 °C for 10 min and the solution replaced. Dopamine was bound to TH by incubating suitable amounts of nonphosphorylated TH with 10 μM dopamine for 20 min at room temperature. Equal amounts of the dopamine-bound TH and 2% OC mixture were combined and incubated for a maximum of 3 min to remove low-affinity bound and free dopamine, while minimizing TH binding to charcoal. The mixture was then centrifuged at 18000g at 4 °C for 5 min and the supernatant kept on ice until required for dose−response experiments, where increasing amounts of dopamine were added back onto the low-affinity site prior to measuring activity (as described above), or kinetic experiments, where the activity of the high-affinity dopamine-bound TH was measured over 0−1500 μM BH_4.

TH Activity Measurements. Measurements of specific activity for dose−response experiments and enzyme kinetics were carried out using the tritiated water release assay based on the methodology of Reinhard et al. (*14*), involving quantitation of product (^3H_2O) from radiolabeled tyrosine. The reaction used phosphorylated or nonphosphorylated TH with concentrations ranging between 0.07 and 1.7 μM chosen so as to not exceed 10% substrate conversion under the specific assay conditions, 24 μM L-tyrosine, 4.8 μCi/mL [3,5-^{3}H]-L-tyrosine, 0.008% (v/v) 2-mercaptoethanol, 36 μg/mL catalase, 2 mM reduced glutathione, 10 mg/mL ovalbumin, and 100 mM potassium phosphate, pH 7.2.

The 100 μL reactions were initiated with the addition of the essential cofactor BH_4 which was dissolved in 5 mM HCl to prevent oxidation. BH_4 (20 μM) was used for dose−response experiments and 1−1500 μM BH_4 for kinetic analyses. The reactions proceeded for 3 min at 30 °C and were stopped by the addition of 700 μL of 7.5% (w/v) charcoal slurry in 1 M HCl. Samples were vortexed immediately and centrifuged at 18000g for 10 min at 30 °C. Supernatant (350 μL) containing ^3H_2O was added to 3 mL of scintillation cocktail and vortexed for 10 s, and radioactivity was counted for 20 min per sample with a scintillation counter. Controls representing background radioactivity were generated by adding 5 mM HCl to the above reaction rather than BH_4. Positive controls representing 100% substrate conversion were generated by directly adding initial amounts of [^{3}H]tyrosine to the scintillation cocktail.

Direct Binding of Dopamine to the High-Affinity Site. Direct binding experiments involved incubating 900 nM TH with 0−500 nM dopamine hydrochloride, 10 nM [^{3}H]dopamine, 10 mg/mL ovalbumin, 5 mM reduced glutathione, and 100 mM potassium phosphate, pH 7.2, for 30 min at room temperature. The 2% OC charcoal slurry was prepared as outlined above, added to TH dopamine solutions in a 1:1 ratio, and gently mixed. After 3 min, mixtures were centrifuged at 18000g at 4 °C for 5 min. Samples of supernatant were then added to 3 mL of scintillation cocktail, vortexed briefly, and counted for 20 min. Background controls contained no TH protein to account for non-TH binding ^{3}H species remaining in the supernatant after charcoal treatment; 100% binding was measured from samples containing 5 μM TH and [^{3}H]dopamine with no cold dopamine.

RESULTS

In examining the crystal structure of TH (*12*), it was found that a relatively small number of side chains which produced the active site surface were suitable for substitution. This was due to the fact that H331, H336, and E376 are required for iron binding (*12*) and therefore catalysis (*15*), and other areas of the active site involve the backbone portion of the amino acid. Those residues chosen for substitution are shown in Figure 7. Residues E332 and Y371 were chosen as their side chains contribute to the active site and are very close to the catalytic iron without being directly involved in its binding. Conservative substitutions E332Q, E332D, and Y371F were generated to assess the roles of their charged and polar qualities on catecholamine inhibition through the high- and low-affinity sites. E332 has been previously shown to play a major role in catalysis (*16*), although the specific substitutions generated here have not been described previously in the context of dopamine inhibition of TH or otherwise. Y371F has been previously generated to indicate a role of this residue in substrate specificity (*17*). F300 constitutes most of the floor of the active site and had previously been substituted with alanine to produce an active enzyme (*18*). Therefore, F300A was generated to assess its importance as a potential hydrophobic contact for catecholamine binding. An alternative substitution at this site, F300Y, was also generated, which places a hydroxyl group in the vicinity of iron. While the aforementioned residues are conserved among the other hydroxylases, phenylalanine hydroxylase (*19*) and tryptophan hydroxylase (*20*), TH contains some nonconserved residues on the outer edges of the active site which may also have a role in catecholamine inhibition. One such residue, L294, protrudes into the catalytic cleft, and its role was probed by two substitutions: L294A removed the hydrophobic chain from the active site, while L294Y involved the addition of a bulky phenol into the active site entrance where catecholamine may bind. The use of this large, nonconservative substitution was justified by its presence in tryptophan hydroxylase at the 294 (equivalent) position (*20*). The A297 residue is unique to TH and

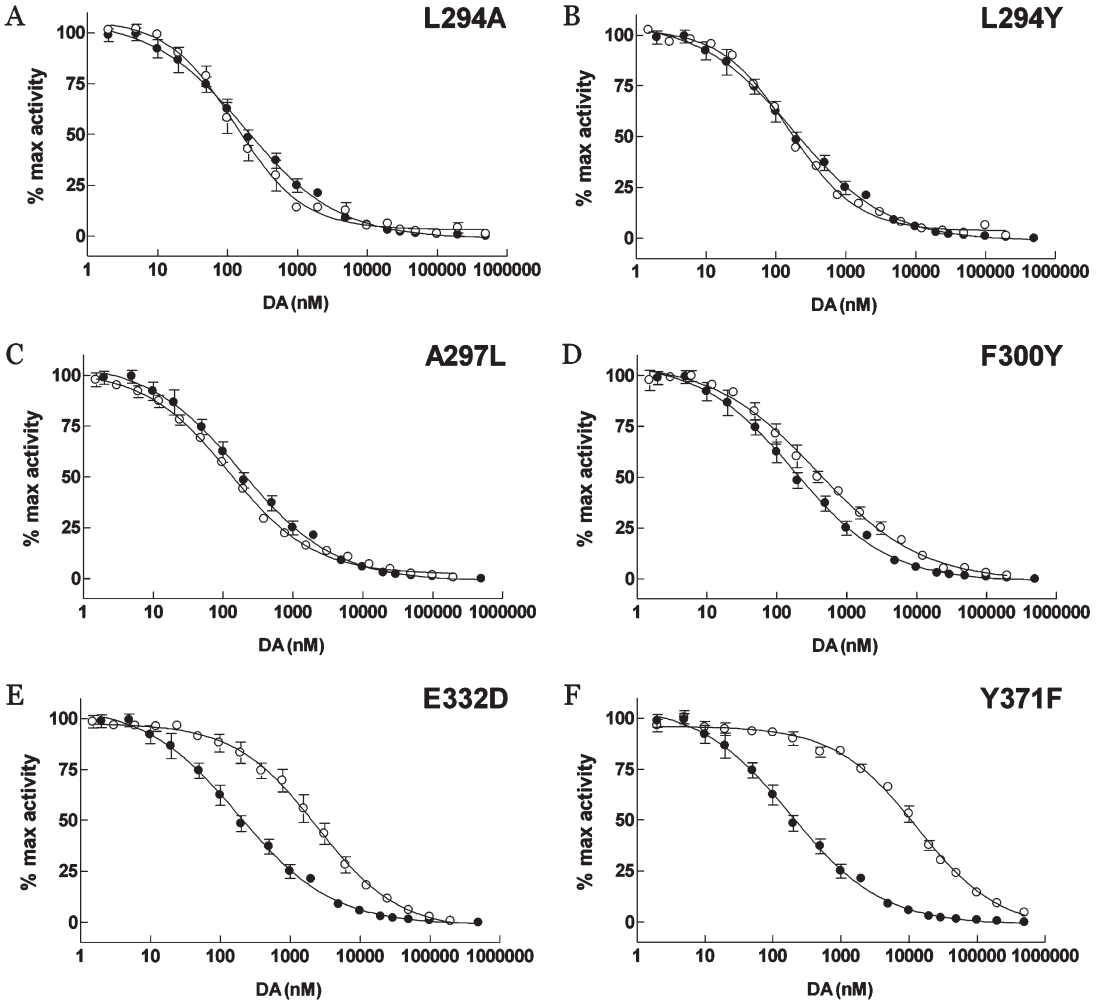

FIGURE 1: Low-affinity site inhibition profiles of phosphorylated wild-type and mutant TH. TH was phosphorylated by PKA, and activity was measured over a range of dopamine concentrations to obtain a value for IC_{50} from a sigmoidal dose−response curve with variable slope. Specific activities are represented as a percentage of the activity measured at 0 nM dopamine within each experiment and are shown as the mean of at least three experiments ± SEM. Wild-type data are shown in each graph (●) alongside mutant data (○). Activities representing 100% for wild-type and mutant TH are shown in Supporting Information.

is located at the outer edge of the active site (*1*). To assess the importance of this region of the active site to catecholamine inhibition, the conservative substitution of A297L was generated. These eight active site mutants were generated and then analyzed for changes to both the low- and high-affinity catecholamine binding sites. First, kinetic analyses were performed to select those mutants with kinetic properties similar to wild-type TH which were suitable to take through this investigation.

BH_4 Kinetic Analyses. Kinetic parameters K_M and V_{max} were obtained by measuring TH activity over a range of BH_4 concentrations. This was done for both the nonphosphorylated and Ser40 phosphorylated forms of TH. Kinetic parameters obtained for wild-type TH were similar to those measured previously (*8*, *9*). These values, along with those obtained for mutant TH, are outlined in Table 2.

All active site mutants had significantly lower values for V_{max} than wild-type TH. The greatest changes were measured for E332Q which had no detectable activity; therefore, an alternative substitution was made at this site (E332D) which resulted in a 10-fold reduction in activity in both the nonphosphorylated and phosphorylated forms. Overall, the catalytic efficiencies (V/K) of the mutants were lower than wild-type TH, ranging from 16% to 30% of the wild-type value in the nonphosphorylated form and 6−24% of the wild-type value in the phosphorylated form. These results indicated modest changes to the enzyme as required. The exception was F300A, whose catalytic efficiency was 3.6% and 1.9% of the wild-type value in the nonphosphorylated and phosphorylated forms, respectively. Values for K_M (BH_4) were of more interest to this study, however; since high- and low-affinity catecholamine binding involves competition with the cofactor, it was desirable to keep the cofactor binding site intact. Generally, nonphosphorylated TH showed minor changes to the K_M for BH_4 (less than 2-fold greater than wild-type and a significantly decreased value for E332D) and were thought to reflect only minor changes to BH_4 binding. Greater changes to the K_M for BH_4 were evident in phosphorylated TH mutants; however, these were still deemed to be suitable for further study, being less than 5-fold greater than the wild-type value. As with the catalytic efficiency, major and undesirable changes to BH_4 binding were evident in F300A, especially in the phosphorylated form where the K_M for BH_4 was over 12-fold larger than that of the wild-type enzyme. Consequently, F300A was not analyzed any further in this study. Remaining active mutants were then analyzed for changes to the low- and high-affinity sites.

Inhibition of TH through the Low-Affinity Site. The specific effects of active site substitutions on the low-affinity

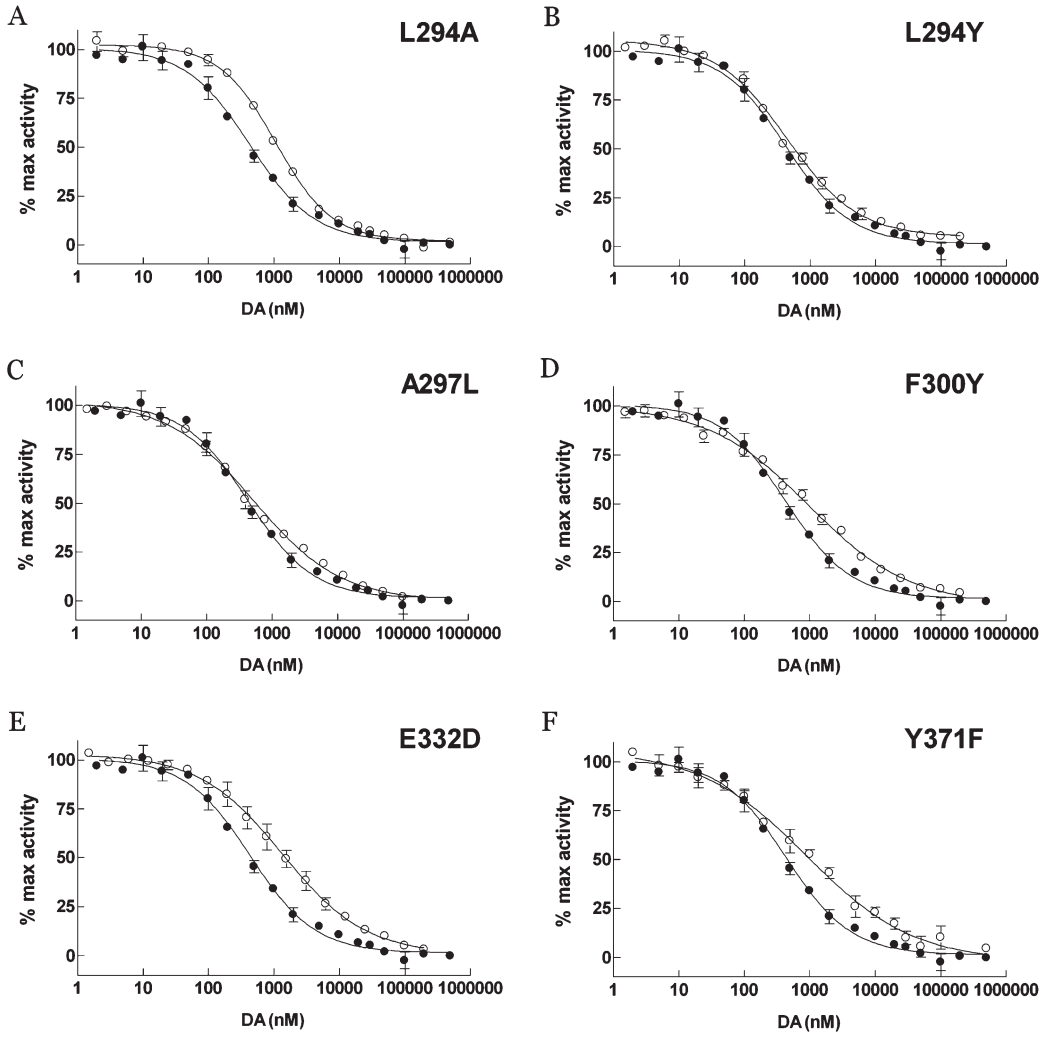

FIGURE 2: Low-affinity site inhibition profiles of nonphosphorylated wild-type and mutant TH. Prior to activity measurements TH was treated with 10 μM dopamine followed by OC charcoal to exclude any high-affinity binding in the experiment. Activity was then measured over a range of dopamine concentrations and a value for IC_{50} obtained from a sigmoidal dose−response curve with variable slope. Specific activities are represented as a percentage of the activity measured at 0 nM dopamine within each experiment and are shown as the mean of at least three experiments ± SEM. Wild-type data are shown in each graph (●) alongside mutant data (○). Activities representing 100% for wild-type and mutant TH are shown in Supporting Information.

catecholamine binding site could be determined by generating dose−response curves where TH activity was measured with increasing concentrations of catecholamine. Dopamine, noradrenaline, and adrenaline have been previously shown to be equivalent in their binding and inhibition of TH (*8*); therefore, dopamine was used as the representative catecholamine in all experiments. When phosphorylated by PKA at Ser40, high-affinity dopamine binding is abolished, and TH is inhibited only through the low-affinity dopamine binding (*8*). As shown in Figure 1, dopamine produces maximal inhibition of phosphorylated wt TH at approximately 10 μM dopamine with half-maximal inhibition, or IC_{50}, occurring at 256 ± 42 nM dopamine. IC_{50} was used as an indicator of changes to the low-affinity site in mutant TH. Of the six mutants tested, only E332D and Y371F displayed significantly different values for IC_{50} when compared to wild-type TH ($p < 0.0001$). The IC_{50} of E332D was 2480 ± 612 nM dopamine (Figure 1E), representing a 10-fold increase in the amount of dopamine required to inhibit wild-type TH. An IC_{50} of 13600 ± 1900 nM dopamine was measured for Y371F (Figure 1F), indicating that 70-fold more dopamine was required to reach the same inhibition as the wild-type enzyme. No significant changes to IC_{50} were measured for the remaining four mutants.

The above data suggest important roles for both E332 and Y371 in low-affinity dopamine binding. However, this effect was measured in phosphorylated TH, which is not necessarily structurally equivalent to the nonphosphorylated form known to have both a high- and a low-affinity site. To measure inhibition through the low-affinity site alone in nonphosphorylated TH, the high-affinity site was saturated with dopamine to prevent any further inhibition through this site in a dose−response experiment. In these experiments both dopamine binding sites are initially saturated with dopamine. Following saturation, ovalbumin-coated charcoal (OC charcoal) binds the free and dissociable dopamine, including that bound to the low-affinity site (see Materials and Methods). TH is left with a saturated and irreversibly bound high-affinity site which does not take part in any further inhibition and an unoccupied low-affinity site which can be assessed in a dose−response experiment. Results from these experiments are shown in Figure 2. Inhibition of wild-type TH through the low-affinity site in the nonphosphorylated form produced an IC_{50} for dopamine inhibition of 400 ± 29 nM. This was a small but significant increase from that measured for phosphorylated TH ($p < 0.05$). Unlike phosphorylated TH, differences in values for IC_{50} between wild-type and mutant TH

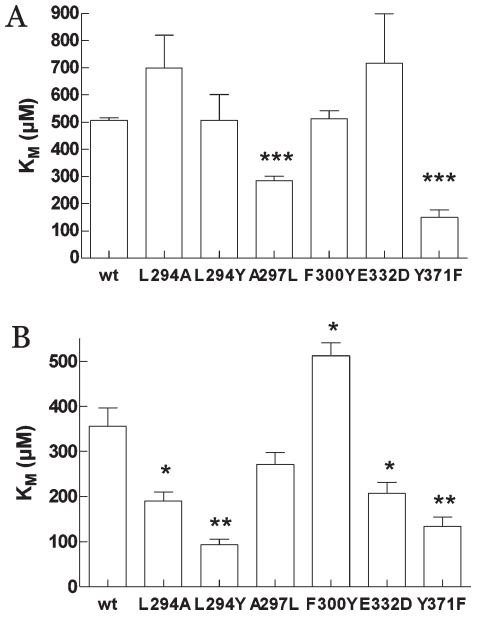

FIGURE 3: Dopamine inhibition through the low-affinity site in wild-type and mutant TH. (A) Phosphorylated TH. (B) Nonphosphorylated TH. For wild-type and mutant TH, values for K_M (BH_4) were calculated from activity assays conducted in the presence of dopamine over a range of BH_4 concentrations (0−1500 μM) as described in Materials and Methods. Values shown represent the mean ± SEM ($N = 3$). Asterisks represent significant differences between wild-type and mutant parameters as measured using Student's t test: *, $p < 0.05$; **, $p < 0.01$; ***, $p < 0.001$.

were modest in the nonphosphoryated form, with four mutants including the aforementioned E332D and Y371F showing small (2−4-fold) but significant increases in the IC_{50} for dopamine as follows: 1070 ± 45 nM for L294A (panel A) ($p < 0.0001$), 930 ± 180 nM for F300Y (panel D) ($p < 0.001$), 1430 ± 500 nM for E332D (panel E) ($p < 0.05$), and 980 ± 150 nM for Y371F (panel F) ($p < 0.01$).

Dose−response experiments revealed those residues important for the affinity of dopamine binding; however, inhibition of TH through the low-affinity site can be analyzed more specifically by directly measuring its competition with the cofactor, BH_4. In a kinetic analysis, the extent of this competition is reflected in the K_M for BH_4 which increases dramatically in the presence of dopamine. Consistent with previously published data (*8*), the K_M for BH_4 in phosphorylated TH increases from the value of 5.6 ± 1 μM in the absence of dopamine (Table 2) to 507 ± 9 μM in the presence of dopamine. In nonphosphorylated TH the K_M for BH_4 increases from 14 ± 1 μM in the absence of dopamine to 356 ± 41 μM in the presence of dopamine. K_M values for mutant TH in the presence of dopamine are shown in Figure 3. Like wild-type TH, all mutants displayed a substantial increase in the K_M for BH_4 in the presence of dopamine, indicating that although increased amounts of dopamine were required for some mutants (as determined from Figures 1 and 2), the ability of low-affinity bound dopamine to disrupt cofactor binding was intact. Small but significant differences in the K_M for BH_4 in the presence of dopamine were measured for the phosphorylated forms of A297L and Y371F (panel A) and for the nonphosphorylated forms of L294A, L294Y, E332D, and Y371F (panel B). This indicates that dopamine bound to the low-affinity site in these mutants does not affect cofactor binding to the extent seen in the wild-type enzyme. This suggests that these mutants cannot position dopamine in the BH_4 binding site as effectively as the wild-type enzyme.

Inhibition of TH through the High-Affinity Site. The high-affinity dopamine binding site was also examined in the active site mutants; however, the unusual nature of this undissociable site required alternative methods for analysis. First, high-affinity binding was measured directly using radiolabeled dopamine. Specifically, nonphosphorylated TH was incubated with a range of [^{3}H]dopamine concentrations for 30 min and treated with OC charcoal which removed all free and low-affinity bound dopamine from solution, leaving TH with varying degrees of high-affinity bound [^{3}H]dopamine. Values for K_D were obtained from the binding curves shown in Figure 4. A K_D of 36.2 ± 5.5 nM dopamine was measured for wild-type TH and was not significantly different to those obtained for L294A, F300Y, E332D, and Y371F, while L294Y and A297L produced significantly higher K_D values of 115 ± 6.3 and 100 ± 1.5 nM, respectively ($p < 0.05$), indicating that these substitutions had reduced the affinity of the high-affinity site for dopamine. The binding data for wild-type TH fitted a sigmoidal saturation model with a Hill coefficient of 1.5 ± 0.15, suggestive of cooperativity of high-affinity dopamine binding. Sigmoidal saturation curves were also fitted to the binding data for F300Y ($h = 1.55 \pm 0.37$) and E332D ($h = 1.31 \pm 0.61$). For L294A, L294Y, A297L, and Y371F, a nonsigmoidal saturation model was chosen over a sigmoidal saturation model as determined by an F-test, indicating that no cooperativity was present.

The effect of dopamine bound to the high-affinity site was also examined by measuring changes in kinetic parameters. A prominent feature of high-affinity dopamine inhibition is its dramatic effect on V_{max}, a mechanism not observed with low-affinity dopamine binding (*8*). Values for V_{max} were obtained from kinetic analyses of nonphosphorylated wild-type and mutant TH in the presence of 10 μM dopamine and are shown in Figure 5. Due to the varied specific activities of the active site mutants, Figure 5 illustrates this inhibition as a percentage of the mutants' corresponding V_{max} in the absence of dopamine. The V_{max} measured for wt TH in the presence of dopamine was very low at 1.02 ± 0.06 min^{-1}, a reduction to 2.8% of the activity of the uninhibited enzyme. Similar reductions were observed with all mutants except A297L and Y371F, whose values for V_{max} were reduced to only 12% and 16% of their uninhibited equivalents, respectively. While this indicates a reduced inhibitory capacity of the high-affinity site in A297L and Y371F, the values of 12% and 16% still reflect a substantial reduction in activity.

In addition to reducing the V_{max}, dopamine binding to the high-affinity site also affects the cofactor by increasing the K_M for BH_4. Nonphosphorylated TH contains both high- and low-affinity sites which independently cause increases in K_M for BH_4 (*8*). Therefore, to assess changes to this feature of the high-affinity site specifically, kinetic analyses were performed on TH with dopamine bound to the high-affinity site alone. OC charcoal was used to generate TH with dopamine bound to the high-affinity site only by removing the free and low-affinity bound dopamine as described earlier. For wild-type TH, it has previously been shown using the OC charcoal procedure (*8*) that dopamine bound to the high-affinity site alone produces a high K_M, measured here as 134 ± 28 μM, indicating that this site disrupts cofactor binding. However, the removal of dopamine from the low-affinity site by OC charcoal allows BH_4 to bind freely, resulting in a second, low K_M of 6.8 ± 1.5 μM in the kinetic profile, similar to that measured in the absence of dopamine as shown in Table 2. The high and low K_M values are obtained by fitting a two-site rather than a one-site saturation model to kinetic

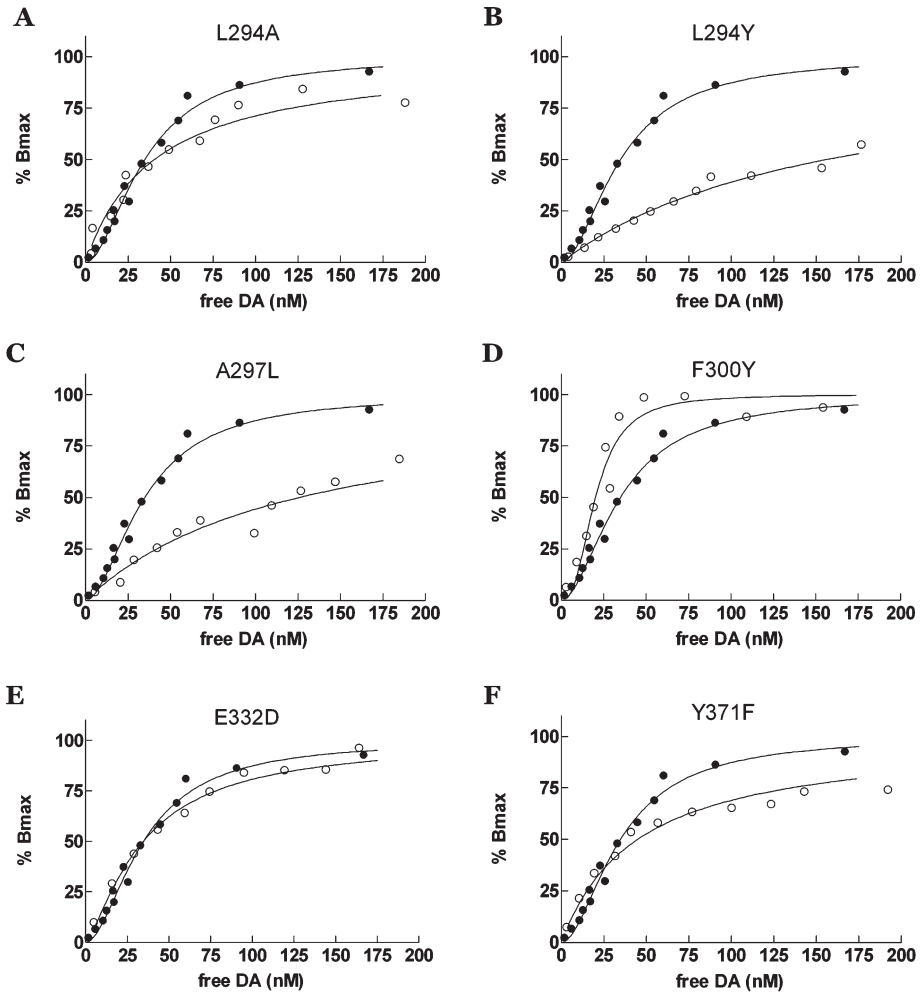

FIGURE 4: Saturation binding of dopamine to the high-affinity site of wuld-type and mutant TH. [^{3}H]Dopamine was allowed to bind TH over 30 min. TH with dopamine bound to the high-affinity site was isolated and measured by removal of free and dissociable dopamine by an ovalbumin-coated charcoal slurry and subsequent scintillation counting of the TH-containing supernatant. Wild-type data are shown in each graph (●) alongside mutant data (○). Data shown are representative plots of three experiments. Due to differences in maximal binding (B_{max}) between wild-type and mutant TH, data have been normalized as a percentage of the B_{max} for visualization purposes. Values for maximal binding for wild-type and mutant TH are shown in Supporting Information. Sigmoidal saturation curves were preferred over saturation binding curves for wt, F300Y, and E332D as determined by *F*-test using GraphPad software.

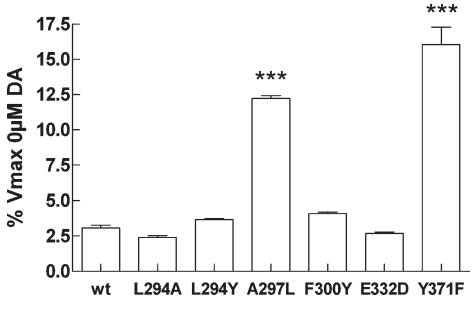

FIGURE 5: Effect of dopamine bound to the high-affinity site on maximal velocity. Wild-type and mutant values for V_{max} were obtained from BH_4 kinetic analyses conducted in the presence of 10 μM dopamine as described in Materials and Methods. Due to the varied specific activities of active site mutants, values for V_{max} in the presence of dopamine have been expressed as a percentage of the V_{max} in the absence of dopamine. Values shown represent the mean ± SEM ($N = 3$). Asterisks represent significant differences between wild-type and mutant parameters as measured using Student's *t* test: *, $p < 0.05$; **, $p < 0.01$; ***, $p < 0.001$.

data and can be visually represented by nonlinear Eadie−Hofstee transformations as shown in Figure 6 with wild-type data in closed circles. Specifically, the steep slope of the Eadie−Hofstee plot in the higher activity region (upper left) corresponds to the high K_M caused by dopamine bound to the high-affinity site, while the shallow slope in the lower activity region (bottom right) is associated with the low K_M caused by the absence of low-affinity bound dopamine. For high-affinity dopamine-bound L294A, L294Y, and F300Y, the resultant high K_M values obtained from a two-site saturation curve were not significantly different from the wild-type value. This is reflected in their Eadie−Hofstee transformations (Figure 6 A,B,D) which coincide with that of wild-type TH in the high K_M region, indicating that the ability of high-affinity bound dopamine to disrupt cofactor binding has been retained in these mutants. The low K_M values of these mutants vary slightly from wild type, as seen in the lower activity regions of the Eadie−Hofstee plots. This is most likely due to the fact that the values for K_M for BH_4 in these mutants are slightly different from wild type in the absence of dopamine (Table 2) and is therefore indicative of small changes to cofactor binding rather than changes to dopamine binding. For high-affinity dopamine-bound A297L (C), E332D (E), and Y371F (F), the Eadie−Hofstee transformations did not coincide with the high K_M region of the wild-type plot; in fact, a two-site saturation model could not

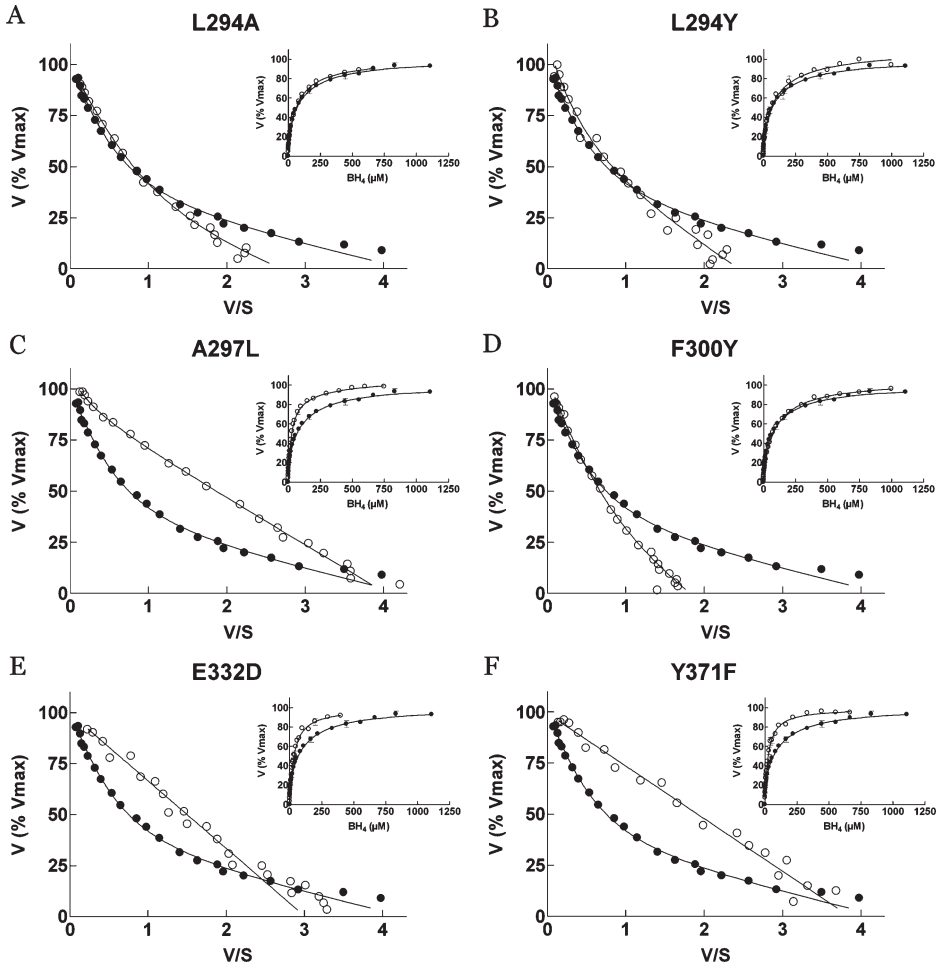

FIGURE 6: Kinetic profiles of high-affinity dopamine-bound wt and mutant TH. After incubation with 10 μM dopamine, TH was treated with OC charcoal and activity measured over a range of BH_4 concentrations which did not produce substrate inhibition. V_{max} and K_M(s) were obtained by fitting a one-site or two-site saturation curve (rectangular hyperbola) to the data from at least three experiments (insert). Wild-type data are shown in each graph (●) alongside mutant data (○). Curved Eadie−Hofstee transformations illustrate the presence of a high and low K_M in wt, L294A, L294Y, and F300Y, while linear Eadie−Hofstee transformations demonstrate the presence of a single, low K_M in A297L, E332D, and Y371F. Data have been expressed as a percentage of the V_{max} to allow visual comparisons with wild-type data.

be fitted to any of the data for these mutants because only a single K_M could be measured in each case, as represented by their linear Eadie−Hofstee transformations. K_M values of 27 ± 2.6 μM for A297L (C), 34 ± 4 μM for E332D (E), and 27 ± 3 μM for Y371F (F) were obtained from a one-site saturation curve. For A297L and Y371F the single K_M was not significantly different to those measured in non-dopamine-bound TH in the phosphorylated and nonphosphorylated forms (Table 2). The value of 34 ± 4 μM in E332D was significantly higher than those of its uninhibited forms ($p < 0.01$); however, it was still significantly lower than the inhibitory wild-type K_M ($p < 0.05$). The absence of a high K_M in A297L, E332D, and Y371F indicates that the high-affinity sites in these mutants no longer have the capacity to disrupt cofactor binding to the extent seen in wild-type TH. For A297L and Y371F especially, this feature of the high-affinity site may have been completely abolished.

DISCUSSION

The high- and low-affinity catecholamine binding sites have been shown to regulate TH simultaneously and independently of each other (*8*). Since both sites disrupt cofactor binding, it is likely that both sites partially overlap the BH_4 binding site. The data shown here confirmed that both high- and low-affinity dopamine binding relies upon some active site residues which act to bind and position dopamine within the BH_4 binding site. Furthermore, the results from this investigation have shown that the high- and low-affinity dopamine binding modes are structurally related, positioned around the iron and anchored by E332 and, to a greater extent, Y371. Other active site resides played minor roles, and A297 was shown to be a key residue for high-affinity dopamine binding only. The structural implications of these findings will now be discussed.

Previous functional characterization of the low-affinity site revealed that its affinity for dopamine was the same in the phosphorylated and nonphosphorylated forms, with comparable K_D values of 60 and 90 nM measured, respectively (*8*). Similarly, the ability of low-affinity bound dopamine to disrupt cofactor binding was found to be the same in the phosphorylated and nonphosphorylated forms (*8*). Based on these findings, it was expected that the low-affinity catecholamine binding sites would be structurally equivalent in phosphorylated and nonphosphorylated TH; however, this was found not to be the case. Here it has been shown that the charged and polar active site residues E332 and Y371 contribute greatly to the low-affinity site in phosphorylated TH, and in nonphosphorylated TH the focus of the site expands to include potential hydrophobic contacts L294 and F300. The structural changes induced by phosphorylation of TH are still not

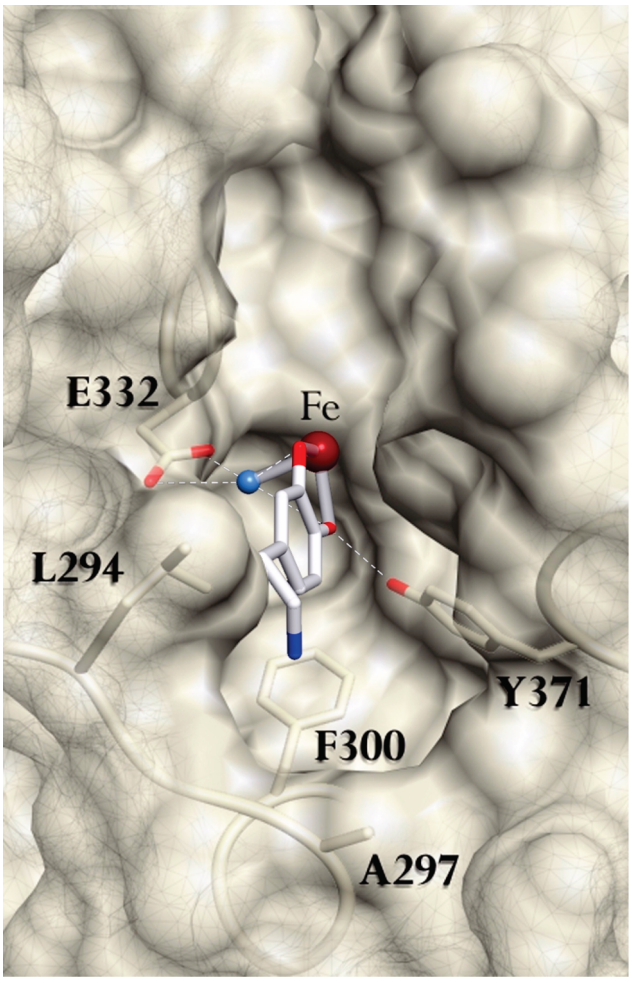

FIGURE 7: Active site residues involved in the low- and high-affinity catecholamine binding sites. Catalytic iron is shown as a red sphere; hydroxyl groups are marked as red sticks, amine groups as blue sticks, and water molecules as blue spheres. This depiction of the active site is based on the crystal structure, 2TOH, with the placement of dopamine and coordinated water molecule based on the dopamine-bound phenylalanine hydroxylase crystal structure, 5PAH, and was generated using UCSF Chimera Version 1.3 and Corel PhotoPaint 11.

completely understood, making it difficult to speculate on what directly causes the apparent structural change to the low-affinity site. The TH crystal structure reveals that E332 and Y371 are located at the back of the active site on either side of the bound iron (*12*) as shown in Figure 7. The position of these residues and their role in low-affinity dopamine binding are consistent with the well-established model of catechol−iron coordination in TH (*6*, *10*), whereby iron-coordinating catechol moieties would be well placed for additional hydrogen bonding with nearby charged/polar components of E332 and Y371. L294 forms a hydrophobic arm over the active site, and it may act to provide an important hydrophobic contact for the dopamine molecule in nonphosphorylated TH only. Addition of a hydroxyl group near the iron on F300 by tyrosine substitution, a similar change to that reported to occur during crystallization (*12*), reduced the affinity of dopamine for the low-affinity site in nonphosphorylated TH only. This result is further evidence that the area surrounding iron plays a role in the affinity of dopamine binding.

Unfortunately, there is no crystal structure of such binding in TH; however, the closely related phenylalanine hydroxylase has been cocrystallized with dopamine (PDB: 5PAH) (*21*) and depicted the expected bidentate catechol−iron coordination with the amino moiety directed into the BH_4 binding site. While this structure provides a model for dopamine binding to TH, it is not clear whether it reflects a high-affinity or low-affinity type of binding. The proposed roles of active site residues in the low-affinity site are consistent with the dopamine-bound PAH structure, especially Y371, whose equivalent in PAH (Y325) provides a stabilizing hydrogen bond to one of the catechol groups of dopamine (*21*). A similar binding is seen in homoprotocatechuate 2,3-dioxygenase (*22*), where the catechol substrate forms bidentate coordinations to His-His-Glu-bound Fe(II) and forms a hydrogen bond with an active site tyrosine in a spatially similar position.

The structural characteristics of high-affinity dopamine binding were also investigated in this study. It is accepted that this type of binding must occur in the active site since it involves coordination with the catalytic iron, and its dependence on phosphorylation suggests a key role of the N-terminus, but involvement of active site residues (if any) has never been elucidated. The key residues previously discussed, E332 and Y371, appear to be involved, in addition to A297. Unlike the low-affinity site, substitutions at E332D and Y371F did not affect the affinity of the high-affinity site for dopamine; rather they reduced the inhibitory capacity of the bound dopamine. The removal of the polar hydroxyl group in Y371F reduced the ability of high-affinity bound dopamine to decrease the V_{max}. Even for the wild-type enzyme, the precise mechanism for V_{max} reduction by dopamine remains to be fully elucidated; however, the iron−catechol coordination is a likely cause. In this case, the proximity of the hydroxyl group of Y371 to iron could provide a means of maintaining catechol−iron coordination. The loss of cofactor competition in Y371F and E332D suggests that their respective high-affinity sites no longer overlap with that of BH_4. If the hydroxyl moiety of Y371 and carboxyl group of E332 do indeed provide a stabilizing hydrogen bond to the bound dopamine molecule as discussed earlier, these may also be important for the high-affinity site, acting as anchors which hold the irreversibly bound dopamine within the BH_4 binding site to exert its inhibition. The importance of A297 to the high-affinity site is interesting, since this residue is located far from Y371 and E332 at the edge of the active site with its side chain directed outward as depicted in Figure 7. Extension of the hydrophobic side chain by leucine substitution reduced the affinity of the high-affinity site for dopamine, an effect also seen with L294Y. These substitutions both involved extensions of the wild-type residues which could possibly impede the entry of dopamine into the active site; however, the resultant reductions in affinity were modest compared to other changes discussed here. A297L had far more dramatic effects on the inhibitory capacity of the high-affinity site, through both mechanisms of V_{max} reduction and cofactor competition. Unlike Y371 and E332, whose roles in high-affinity dopamine binding are probably direct, the peripheral position of A297 suggests its role may be indirect, perhaps by acting as an N-terminal interacting surface essential for correct dopamine positioning and iron coordination. Interestingly, A297 is one of the few active site residues that is not conserved among the hydroxylases, with a serine and proline located at the equivalent residues in PAH and TPH, respectively (*19*, *20*).

The results presented here indicate that residues E332 and Y371 contribute greatly to both the low- and high-affinity catecholamine binding sites. The restricted space around E332 and Y371 colocalizes these two catecholamine binding modes to the iron-bound region of the active site. Colocalization of the

high- and low-affinity sites would be an acceptable conclusion if their binding of catecholamine was mutually exclusive; however, this is not the case. Catecholamines bind to these sites simultaneously, and their effects on the cofactor are not additive, but separate (*8*). The quaternary structure of the TH enzyme, which is in fact a dimer of dimers, raises the possibility that the high- and low-affinity sites may be spread over two monomers of TH, where one monomer of the dimer binds catecholamine with high affinity and the other monomer binds catecholamine with low affinity. This model is consistent with stoichiometries of dopamine binding measured previously in nonphosphorylated TH, where values approaching 1 mol of dopamine/mol of TH dimer were obtained for the each of the high- and low-affinity sites (*8*). In phosphorylated TH where only low-affinity sites exist, the stoichiometry has been measured as approximately 2 mol of dopamine/mol of TH dimer (*8*). This implies that upon phosphorylation a low-affinity site takes the place of the high-affinity site. So while the catalytic unit of TH is considered to be the monomer (*2*), this may not be true for the "regulatory unit" of a high- and low-affinity dopamine binding site. This regulatory unit is therefore proposed as an asymmetric dimer containing one high-affinity binding site, and one low-affinity binding site, which loses asymmetry upon phosphorylation to produce two low-affinity binding sites. Currently, there is not enough structural information on TH to explain the asymmetry that produces the two binding sites. Both TH crystal structures produced to date show that monomers are structurally equivalent within the tetramer (*1*); however, these structures contain iron in the ferric form and are lacking the N-terminal 156 amino acids. If binding to ferric iron is a determinant for the high-affinity site, the presence of a colocalized low-affinity site may be due to a weaker interaction with the catalytically active ferrous iron. The lack of V_{MAX} reduction in low-affinity binding is suggestive of an interaction with ferrous iron, but it is yet to be directly shown. Catechol binding to ferrous iron is certainly possible and is known to underlie the mechanism of substrate binding in the extradiol dioxygenases, including the aforementioned homoprotocatechuate 2,3-dioxygenase (*22*, *23*). In TH, high- and low-affinity binding cannot be generated by a switching of ferric to ferrous iron in the one active site, however; otherwise, high-affinity bound catecholamine would easily dissociate. They must exist in separate active sites. Considering the absolute requirement for the N-terminus on high-affinity catecholamine binding and the effect of phosphorylation, this as yet uncrystallized region of TH may be responsible for the asymmetry across the TH dimer through an asymmetrical folding among subunits, for example. There is some evidence for this; phosphorylation at Ser31 does not exceed 1 mol of phosphate/mol of TH dimer (*24*), indicating that only one subunit in the dimer contains an accessible residue at this site. Further studies involving dopamine inhibition in dimeric and monomeric TH are being undertaken in our laboratory to investigate the importance of this enzyme's quaternary structure in regulation by the catecholamines.

While the results described here have partially revealed the structural basis of catecholamine inhibition of TH, they have hinted at a far more complex process which extends beyond the active site and indeed may depend on the entire tetramer.

ACKNOWLEDGMENT

We thank Peter Dunkley and John Rostas for critically reading the manuscript.

SUPPORTING INFORMATION AVAILABLE

Values for specific activities representing 100% in dose−response experiments from phosphorylated and OC charcoal treated TH and values for maximal binding of dopamine to the high-affinity site in wild-type and mutant TH. This material is available free of charge via the Internet at http://pubs.acs.org.

REFERENCES

1. Goodwill, K. E., Sabatier, C., Marks, C., Raag, R., Fitzpatrick, P. F., and Stevens, R. C. (1997) Crystal structure of tyrosine hydroxylase at 2.3 Å and its implications for inherited neurodegenerative diseases. *Nat. Struct. Biol. 4*, 578–585.
2. Fitzpatrick, P. F. (2003) Mechanism of aromatic amino acid hydroxylation. *Biochemistry 42*, 14083–14091.
3. Eser, B. E., Barr, E. W., Frantom, P. A., Saleh, L., Bollinger, J. M., Jr., Krebs, C., and Fitzpatrick, P. F. (2007) Direct spectroscopic evidence for a high-spin Fe(IV) intermediate in tyrosine hydroxylase. *J. Am. Chem. Soc. 129*, 11334–11335.
4. Grima, B., Lamouroux, A., Boni, C., Julien, J. F., Javoy-Agid, F., and Mallet, J. (1987) A single human gene encoding multiple tyrosine hydroxylases with different predicted functional characteristics. *Nature 326*, 707–711.
5. Dunkley, P. R., Bobrovskaya, L., Graham, M. E., von Nagy-Felsobuki, E. I., and Dickson, P. W. (2004) Tyrosine hydroxylase phosphorylation: regulation and consequences. *J. Neurochem. 91*, 1025–1043.
6. Andersson, K. K., Cox, D. D., Que, L., Jr., Flatmark, T., and Haavik, J. (1988) Resonance Raman studies on the blue-green-colored bovine adrenal tyrosine 3-monooxygenase (tyrosine hydroxylase). Evidence that the feedback inhibitors adrenaline and noradrenaline are coordinated to iron. *J. Biol. Chem. 263*, 18621–18626.
7. McCulloch, R. I., Daubner, S. C., and Fitzpatrick, P. F. (2001) Effects of substitution at serine 40 of tyrosine hydroxylase on catecholamine binding. *Biochemistry 40*, 7273–7278.
8. Gordon, S. L., Quinsey, N. S., Dunkley, P. R., and Dickson, P. W. (2008) Tyrosine hydroxylase activity is regulated by two distinct dopamine-binding sites. *J. Neurochem. 106*, 1614–1623.
9. Daubner, S. C., Lauriano, C., Haycock, J. W., and Fitzpatrick, P. F. (1992) Site-directed mutagenesis of serine 40 of rat tyrosine hydroxylase. Effects of dopamine and cAMP-dependent phosphorylation on enzyme activity. *J. Biol. Chem. 267*, 12639–12646.
10. Almas, B., Le Bourdelles, B., Flatmark, T., Mallet, J., and Haavik, J. (1992) Regulation of recombinant human tyrosine hydroxylase isozymes by catecholamine binding and phosphorylation. Structure/activity studies and mechanistic implications. *Eur. J. Biochem. 209*, 249–255.
11. Gordon, S. L., Webb, J. K., Shehadeh, J., Dunkley, P. R., and Dickson, P. W. (2009) The low affinity dopamine binding site on tyrosine hydroxylase: the role of the N-terminus and in situ regulation of enzyme activity. *Neurochem. Res. 34*, 1830–1837.
12. Goodwill, K. E., Sabatier, C., and Stevens, R. C. (1998) Crystal structure of tyrosine hydroxylase with bound cofactor analogue and iron at 2.3 Å resolution: self-hydroxylation of Phe300 and the pterin-binding site. *Biochemistry 37*, 13437–13445.
13. Bevilaqua, L. R., Graham, M. E., Dunkley, P. R., von Nagy-Felsobuki, E. I., and Dickson, P. W. (2001) Phosphorylation of Ser(19) alters the conformation of tyrosine hydroxylase to increase the rate of phosphorylation of Ser(40). *J. Biol. Chem. 276*, 40411–40416.
14. Reinhard, J. F., Jr., Smith, G. K., and Nichol, C. A. (1986) A rapid and sensitive assay for tyrosine-3-monooxygenase based upon the release of ^3H_2O and adsorption of [^{3}H]-tyrosine by charcoal. *Life Sci. 39*, 2185–2189.
15. Fitzpatrick, P. F., Ralph, E. C., Ellis, H. R., Willmon, O. J., and Daubner, S. C. (2003) Characterization of metal ligand mutants of tyrosine hydroxylase: insights into the plasticity of a 2-histidine-1-carboxylate triad. *Biochemistry 42*, 2081–2088.
16. Daubner, S. C., and Fitzpatrick, P. F. (1999) Site-directed mutants of charged residues in the active site of tyrosine hydroxylase. *Biochemistry 38*, 4448–4454.
17. Daubner, S. C., and Fitzpatrick, P. F. (1998) Mutation to phenylalanine of tyrosine 371 in tyrosine hydroxylase increases the affinity for phenylalanine. *Biochemistry 37*, 16440–16444.
18. Ellis, H. R., Daubner, S. C., McCulloch, R. I., and Fitzpatrick, P. F. (1999) Phenylalanine residues in the active site of tyrosine hydroxylase: mutagenesis of Phe300 and Phe309 to alanine and metal ion-catalyzed hydroxylation of Phe300. *Biochemistry 38*, 10909–10914.

19. Erlandsen, H., Fusetti, F., Martinez, A., Hough, E., Flatmark, T., and Stevens, R. C. (1997) Crystal structure of the catalytic domain of human phenylalanine hydroxylase reveals the structural basis for phenylketonuria. *Nat. Struct. Biol. 4*, 995–1000.
20. Wang, L., Erlandsen, H., Haavik, J., Knappskog, P. M., and Stevens, R. C. (2002) Three-dimensional structure of human tryptophan hydroxylase and its implications for the biosynthesis of the neurotransmitters serotonin and melatonin. *Biochemistry 41*, 12569–12574.
21. Erlandsen, H., Flatmark, T., Stevens, R. C., and Hough, E. (1998) Crystallographic analysis of the human phenylalanine hydroxylase catalytic domain with bound catechol inhibitors at 2.0 Å resolution. *Biochemistry 37*, 15638–15646.
22. Fielding, A. J., Kovaleva, E. G., Farquhar, E. R., Lipscomb, J. D., and Que, L., Jr. (2011) A hyperactive cobalt-substituted extradiol-cleaving catechol dioxygenase, *J. Biol. Inorg. Chem.* (DOI 10.1007/s00775-010-0732-0).
23. Arciero, D. M., and Lipscomb, J. D. (1986) Binding of ^{17}O-labeled substrate and inhibitors to protocatechuate 4,5-dioxygenase-nitrosyl complex. Evidence for direct substrate binding to the active site Fe^{2+} of extradiol dioxygenases. *J. Biol. Chem. 261*, 2170–2178.
24. Lehmann, I. T., Bobrovskaya, L., Gordon, S. L., Dunkley, P. R., and Dickson, P. W. (2006) Differential regulation of the human tyrosine hydroxylase isoforms via hierarchical phosphorylation. *J. Biol. Chem. 281*, 17644–17651.